


Article

# Outage Constrained Design in NOMA-Based D2D Offloading Systems

Yun Chen <sup>1,2</sup> , Guoping Zhang <sup>1,\*</sup>, Hongbo Xu <sup>1</sup>, Yinshuan Ren <sup>2</sup>, Xue Chen <sup>1</sup> and Ruijie Li <sup>1</sup>

<sup>1</sup> The College of Physical Science and Technology, Central China Normal University of China, Wuhan 430079, China; cy2020@mails.ccn.u.edu.cn (Y.C.); xuhb@mail.ccn.u.edu.cn (H.X.); chenxue@mails.ccn.u.edu.cn (X.C.); rjli2020@mails.ccn.u.edu.cn (R.L.)

<sup>2</sup> The School of Physics and Electronics, Qiannan Normal University for Nationalities, Duyun 558000, China; renyinshuan318@163.com

\* Correspondence: gpzhang@mail.ccn.u.edu.cn

**Abstract:** Non-orthogonal multiple access (NOMA) is a new multiple access method that has been considered in 5G cellular communications in recent years, and can provide better throughput than traditional orthogonal multiple access (OMA) to save communication bandwidth. Device-to-device (D2D) communication, as a key technology of 5G, can reuse network resources to improve the spectrum utilization of the entire communication network. Combining NOMA technology with D2D is an effective solution to improve mobile edge computing (MEC) communication throughput and user access density. Considering the estimation error of channel, we investigate the power of the transmit nodes optimization problem of NOMA-based D2D networks under the rates outage probability (OP) constraints of all single users. Specifically, under the channel statistical error model, the total system transmit power is minimized with the rate OP constraint of a single device. Unfortunately, the problem presented is thorny and non-convex. After equivalent transformation of the rate OP constraints by the Bernstein inequality, an algorithm based on semi-definite relaxation (SDR) can efficiently solve this challenging non-convex problem. Numerical results show that the channel estimation error increases the power consumption of the system. We also compare NOMA with the OMA mode, and the numerical results show that the D2D offloading systems based on NOMA are superior to OMA.

**Keywords:** power optimization; Internet of Things (IoT); non-orthogonal multiple access (NOMA); outage probability; D2D transmission



**Citation:** Chen, Y.; Zhang, G.; Xu, H.; Ren, Y.; Chen, X.; Li, R. Outage Constrained Design in NOMA-Based D2D Offloading Systems. *Electronics* **2022**, *11*, 256. <https://doi.org/10.3390/electronics11020256>

Academic Editor: Wojciech Mazurczyk

Received: 13 November 2021

Accepted: 11 January 2022

Published: 13 January 2022

**Publisher's Note:** MDPI stays neutral with regard to jurisdictional claims in published maps and institutional affiliations.



**Copyright:** © 2022 by the authors. Licensee MDPI, Basel, Switzerland. This article is an open access article distributed under the terms and conditions of the Creative Commons Attribution (CC BY) license (<https://creativecommons.org/licenses/by/4.0/>).

## 1. Introduction

With the development of Internet of Things (IoT) technology and the diversification of mobile communication services, people's dependence on intelligent devices is increasing. However, with the increase in the number of intelligent terminal devices, people's business needs become more and more frequent, and their requirements for data throughput become higher, which makes the scarce spectrum resources more strained [1,2]. Therefore, it is necessary to improve the capacity and spectral efficiency of communication networks to support the growing communication services while ensuring their performance [3,4]. As an essential technology in 5G communication systems, device-to-device (D2D) networking has been studied extensively. In D2D communication networks, devices can communicate directly with each other by reusing cellular user resources. This D2D scheme not only reduces the base station (BS) and server workload, but also improves the spectrum efficiency of the communication system [5,6]. In recent years, mobile edge computing (MEC) has become a task-intensive application that reduces computing latency by utilizing local and edge computing on the device [7]. However, the computing resources and capacity of edge servers are limited, so we need to find ways to reduce the heavy computing burden.

Therefore, D2D communication is adopted to reduce the burden of edge servers through user cooperative offloading [8–11].

The D2D network, as a vision technology of the next generation communication system, can increase coverage, resource reuse, data transmission with high rate and low delay, and support many applications, such as mobile cloud computing and resource sharing [12]. D2D technology has been considered for the ultra-dense network of collaborative positioning, and is expected to achieve ubiquitous positioning with an accuracy of less than one meter to meet the 5G requirements. The authors of [13] analyzed the advantages and disadvantages of D2D as an enabling technology for cooperative cellular localization. The authors of [14,15] adopted different algorithms to allocate channels and control power with the goal of improving the energy efficiency of devices. The authors of [16] studied D2D networks resource allocation schemes to minimize the power consumption of cellular users and D2D users. The authors of [17] adopted deep learning to solve the prediction problem of D2D channel gain. The authors of [18] aimed at minimizing latency in intelligent reflecting surface (IRS) assisted D2D offloading systems by jointly [19] optimizing IRS phase shift and resource allocation algorithm. In [19], the authors adopted an iterative algorithm to realize the optimal power distribution to maximize the energy efficiency of D2D networks. To improve the energy efficiency of D2D networks, the authors in [20] proposed a joint power resource allocation method in deploying D2D networks to improve system throughput, users service quality, and power consumption. The authors of [21] proposed an optimization algorithm combining energy collection, time slot allocation, power and spectrum iteration to maximize the energy efficiency of D2D networks.

In addition, apart from using D2D to optimize the spectral efficiency of wireless networks, another essential technique, non-orthogonal multiple access (NOMA), can also able to improve the spectral efficiency and increase system coverage. The authors of [22] first discovered NOMA's potential in 5G networks and verified that NOMA is superior to OMA in channel capacity and user fairness. NOMA is considered one of the promising new technologies in future 5G networks, as it can dramatically improve the efficiency of the communication spectrum [23]. Unlike previous multi-access technologies, NOMA's basic idea is that users can transmit data in the same frequency band over the same time slot, and the data sent to different users can be distinguished by different transmission power levels. In particular, the advantages are more evident in the case of power domain multiplexing NOMA, allowing multiple users to share spectrum resources and using serial interference elimination (SIC) technology to achieve multi-user detection. Although NOMA increases the complexity of the receiver compared with traditional orthogonal multiple access (OMA), it significantly improves the frequency spectrum utilization of the communication system.

As described in Figure 1, the base station sends two superimposed user signals, and the link gain of device 2 is higher than that of device 1 in a NOMA communication system. Downlink NOMA assigns higher transmit power to users with poor link gain and lower transmit power to users with good link gain. With the SIC method, the user's signal with the highest transmitting power is decoded first, followed by the second most powerful signal, and so on until all signals are separated.

So far, there have been a lot of studies on NOMA in different application scenarios. The authors of [24] maximized the system sum rate by jointly optimizing user-subchannel allocation and users' power allocation. The authors of [25] improved the data throughput of NOMA-based systems by optimizing the subcarrier power allocation scheme. Assuming perfect instantaneous CSI, the authors of [26] adopted the MIMO-NOMA framework to study the method of eliminating interference between clusters. The authors of [27] innovatively proposed a NOMA scheme for large-scale MIMO systems considering finite feedback channels. However, D2D technology or NOMA technology was used alone in the above research scenarios. Due to the popularization of IoT, large-scale access will further aggravate the spectrum congestion of communication network. We propose to combine NOMA technology with D2D technology, which can significantly improve the performance of IoT systems.

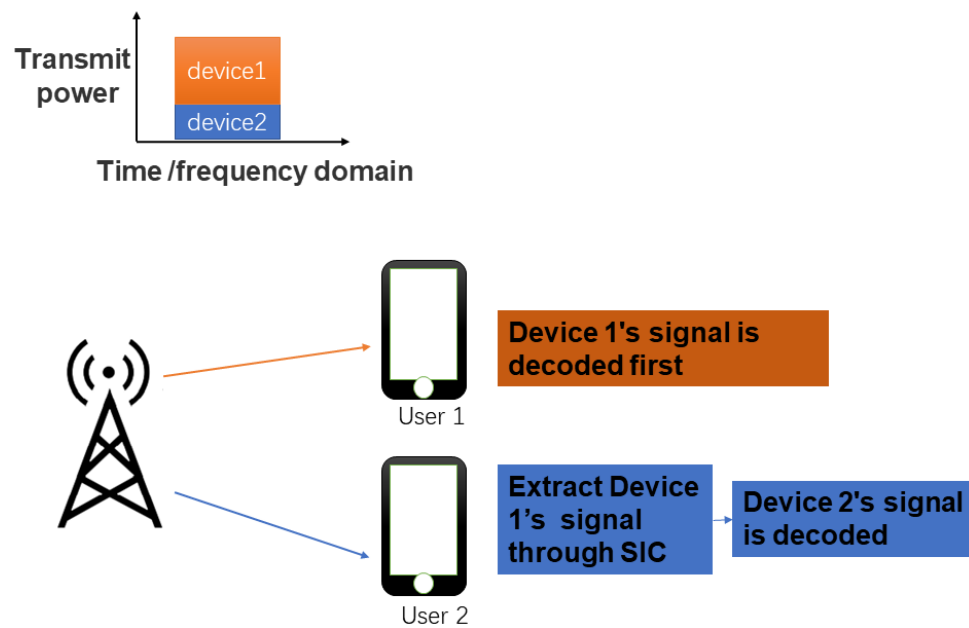


**Figure 1.** Downlink NOMA network with two users.

### 1.1. Related Works

Large-scale D2D communication will further aggravate spectrum congestion in communication networks. NOMA can easily integrate existing advanced solutions, such as Internet of Things (IoT) [28] and D2D communications [29]. Combining NOMA technology with D2D technology can significantly improve the performance of the D2D network. The basic idea of NOMA-based D2D is to allow the receiver to access data over the same time slot and the same frequency band via transmitters by superimposed encoding. Then, using SIC technology, each user of the D2D system can accurately extract data from the superposition signal [29].

The authors of [30] optimized subchannel allocation and power control to maximize the throughput of the D2D system and applied NOMA technology in D2D links to maximize spectral efficiency. The authors of [31] studied the full-duplex D2D assisted mm-Wave NOMA networks and derived closed expressions for (outage probability) OP and traversal capacity. In [32], with sharing spectrum resources through NOMA, power control allocation was optimized to maximize the total rate of D2D user pairs while ensuring users' rate constraints. The authors of [33] studied the integration model of NOMA and D2D communication and further deduced the expression of OP that both users in NOMA get high rate under the fixed power constraint. The authors in [10] studied the NOMA-based D2D-assisted MEC systems by deploying a D2D network to realize user collaboration and reduce the load of edge servers. The transmitters in the D2D system send data to the receivers simultaneously through NOMA technology, the authors of [34] summarized an effective power distribution algorithm which effectively solves the resource allocation problem of the NOMA-based D2D communication system. Based on a fixed power allocation strategy, the authors of [35] derived the closed expressions of OP and traversal capacity of D2D NOMA in both complete and incomplete SIC cases. The authors of [36] derived the closed-form expressions of ergodic sum rate, OP without eavesdropper, and secrecy rate with an eavesdropper in D2D-NOMA systems, respectively.

### 1.2. Main Contributions

Until now, most of the research works on NOMA-based D2D networks have assumed that channel status information (CSI) is completely known. However, in some practical application scenarios, it is hard to obtain the perfect CSI of communication system. Channel estimation error has a close influence on system performance. Therefore, it is of great significance to study parameter optimization of NOMA-based D2D network systems under

imperfect CSI. The authors of [37] proposed that the power used to transmit signals by IoT devices is much greater than the power used to collect data. Since mobile devices in D2D networks are battery powered, D2D communication can minimize the power consumption of devices during data transmission to prolong the life cycle of devices. The main contributions of the work are summarized as follows:

- (1) In MEC, D2D communication technology is adopted to reduce the burden of edge servers through user cooperative offloading.
- (2) Due to the inevitable CSI estimation error, the total transmit power minimization problem of D2D systems is established subject to individual rate OP constraints under the imperfect CSI model. Here, the rate OP constraint represents the probability that each user’s rate reaches its minimum rate requirement with a probability greater than the preset probability.
- (3) The problem formulated is non-convex, and it is hard to tackle. The equivalent transformation of the rate OP is carried out using the Bernstein inequality, and then the reformulated problem can be efficiently solved by semi-definite relaxation (SDR).
- (4) The numerical results show that the level of statistical error has a great influence on the performance of the NOMA-based D2D system. Specifically, the total transmitted power decreases as the error decreases. The numerical results also verify that the system power consumption of D2D with NOMA is better than OMA.

The rest of the work is arranged as follows. Section 2 describes the signal model and channel uncertainty model. Then, the power optimization problem subject to the rates outage probability (OP) constraint and its solution method are described in detail in Section 3. We analyze the simulation results in Section 4. Finally, Section 5 shows the conclusion of this article.

Notations: We use a bold lowercase letter and bold uppercase letter to define the vector and matrices, respectively.  $\|\bullet\|_F$  and  $\|\bullet\|$  denote the Frobenius norm of the matrix and Euclidean norm of a vector, respectively.  $X^H$  denotes the Hermitian of a matrix  $X$ .  $X \succeq 0$  means that  $X$  is positive semi-definite. The trace of the matrix is defined by  $Tr\{\bullet\}$ . The complex and real field are described as  $\mathbb{C}$  and  $\mathbb{R}$ , respectively. In addition,  $\lambda_{max}(\cdot)$  and  $\lambda(\bullet)$  denote the maximum eigenvalue and eigenvalue of the matrix, respectively.

## 2. System Model

In this paper, we analyze the D2D communication system based on NOMA, and we assume that the SIC process of D2D communication based on NOMA is perfect. As shown in Figure 2, there are  $L$  D2D link pairs in the system. We denote by  $g_l \in \mathbb{C}$  the link coefficient from transmitter  $DT_l$  to receiver  $DR_l$ , where  $l \in \mathcal{L} = 1, 2, \dots, L$ .

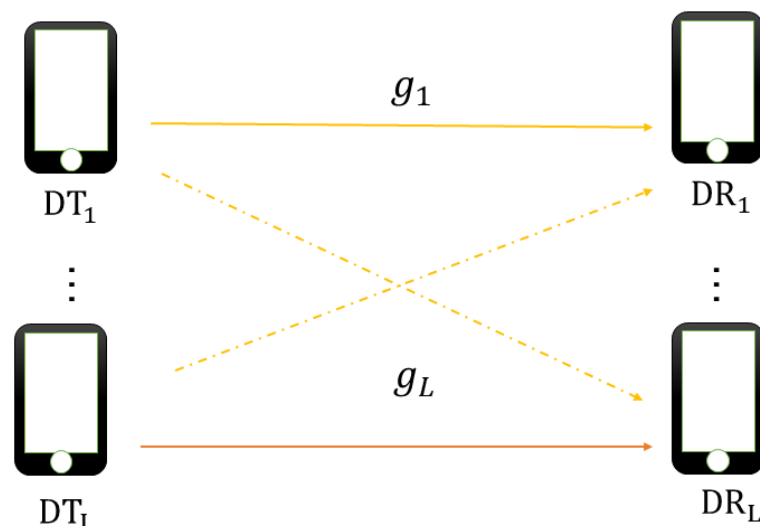


Figure 2. System model for the NOMA-based D2D communication system with  $L$  D2D links.

### 2.1. Signal Model

The transmit data for user  $DT_l$   $x_l$  are assumed to have unit variance, i.e.,  $E(x_l x_l^H) = 1$ . We denote the transmit power of D2D link  $l$  by  $p_l$ . The received signal of  $DR_l$  is as follows:

$$y_l = \sum_{i=1}^L g_l^H \sqrt{p_i} x_i + n, \tag{1}$$

where  $n \in \mathbb{C} \mathcal{CN}(0, \sigma^2)$  is the channel noise vector, and the signal-to-interference-plus-noise ratio (SINR) of link  $l$  in the NOMA-based D2D communication network can be expressed as

$$z_l = \frac{|g_l^H|^2 p_l}{\sum_{i=l+1}^L |g_l^H|^2 p_i + \sigma^2}. \tag{2}$$

Then, the achievable rate of link  $l$  is given by

$$R_l = B \log_2 \left( 1 + \frac{|g_l^H|^2 p_l}{\sum_{i=l+1}^L |g_l^H|^2 p_i + \sigma^2} \right), \tag{3}$$

where  $B$  is the communication bandwidth of D2D systems.

### 2.2. Channel Uncertainty Model

In D2D communication systems, it is impossible to transmit the infinite feedback information containing large numbers of signals between the transmitter and receiver, so it is difficult to obtain perfect CSI. We assume that the channel between users is imperfect, which is represented as

$$g_l = \hat{g}_l + \Delta g_l, \tag{4}$$

where  $\hat{g}_l$  is the estimated channel vector, and  $\Delta g_l$  is the corresponding channel estimation error vector.

In this paper, we consider the CSI statistical error model. Specifically, all CSI errors are assumed to satisfy the i.i.d. complex Gaussian distributed entries, i.e.,

$$vec(\Delta g_l) \sim \mathcal{CN}(0, \Sigma_l), \Sigma_l \succcurlyeq 0, \forall l \in \mathcal{L}, \tag{5}$$

where  $\Sigma_l \in \mathbb{C}$  is positive semi-definite error covariance matrices.

## 3. Problem Formation and Solution

### 3.1. Problem Formulation

In this paper, we aim to optimize the total system transmit power of the NOMA-based D2D communication network under the individual rate OP constraints at the users. Specifically, under the channel statistical error model, the total system transmit power is minimized with the rate OP of a single device as a constraint. The total transmit power of the NOMA-based D2D communication network can be expressed as follows:

$$p_{total} = \sum_{l=1}^L p_l. \tag{6}$$

The rate OP of the system users can be defined as the following expression:

$$Pr \left\{ \text{Blog}_2 \left\{ 1 + \frac{|g_l^H|^2 p_l}{\sum_{i=l+1}^L |g_i^H|^2 p_i + \sigma^2} \right\} \geq r_l \right\} \geq 1 - \rho_l, \tag{7}$$

where  $r_l$  is the minimal target rate for user  $l$ , and  $\rho_l$  is the OP threshold.

According to Equations (6) and (7), the optimization problem is summarized as the following expression:

$$\min_p \sum_{l=1}^L p_l \tag{8a}$$

$$\text{s.t. C1 : } Pr\{R_l \geq r_l\} \geq 1 - \rho_l, \forall l \in \mathcal{L} \tag{8b}$$

$$p_i \geq p_l, \forall i < l \tag{8c}$$

$$|g_1^H| \leq \dots \leq |g_L^H|. \tag{8d}$$

Note that constraints (8b) are the individual rate outage constraint, which ensures that the rate OP of the user should be smaller than the threshold  $\rho_l$  in the presence of channel estimation errors. It should be noted that the occurrence of rate outages is not only related to the CSI estimation error, but also to the poor link quality itself. In the NOMA transmission mode, higher transmission power is assigned to the user with poor link gain, and lower transmission power is assigned to the user with good link gain to ensure correct decoding at the receiver. Constraints (8c) and (8d) ensure that the users can correctly decode the received information during NOMA using the SIC method.

The difficulty in solving problem (8) lies mainly in the constraint (8b), because (8b) is only a probability form. The closed expression for OP can be obtained using the method described in [38]. To make problem (8) easy to solve, we suggest a new way to deal with (8b). Specifically, we would firstly transform (8b) into an equivalent tractable formulation. In the next subsection, we propose specific solutions to problem (8).

### 3.2. Beamforming Design

Solving problem (8) is complicated due to the non-convex constraints (8b). Thus, we would first use the Bernstein inequality to transform constraints (8b) into an equivalent and tractable form. Specifically, an equivalent transformation based on the Bernstein inequality is described in Lemma 1.

**Lemma 1** (Bernstein inequality [39]). Assume  $F(\mathbf{s}) = \mathbf{s}^H \mathbf{U} \mathbf{s} + 2\text{Re}\{\mathbf{u}^H \mathbf{s}\} + v$ , where  $\mathbf{U} \in \mathbb{H}^{n \times n}$ ,  $\mathbf{u} \in \mathbb{C}^{n \times 1}$ ,  $v \in \mathbb{R}$  and  $\mathbf{s} \in \mathbb{C}^{n \times 1} \sim \mathcal{CN}(0, I)$ . Then for any  $\delta \in [0, 1]$ , the following transformation holds:

$$\begin{aligned} & Pr\{\mathbf{s}^H \mathbf{U} \mathbf{s} + 2\text{Re}\{\mathbf{u}^H \mathbf{s}\} + v \geq 0\} \geq 1 - \delta \\ \Rightarrow & \text{Tr}\{\mathbf{U}\} - \sqrt{2\ln(1/\delta)}s + \ln(\delta)\lambda_{\max}^+(-\mathbf{U}) + v \geq 0 \\ \Rightarrow & \begin{cases} \text{Tr}\{\mathbf{U}\} - \sqrt{2\ln(1/\delta)}s + \ln(\delta)t + v \geq 0 \\ \sqrt{\|\mathbf{U}\|_F^2 + 2\|\mathbf{u}\|^2} \leq s \\ tI + \mathbf{U} \succcurlyeq 0, t \geq 0, \end{cases} \end{aligned} \tag{9}$$

where  $\lambda_{\max}^+(-\mathbf{U}) = \max(\lambda_{\max}(-\mathbf{U}), 0)$ .  $s$  and  $t$  are slack variables.

Before the transformations, the rate OP constraint of link  $l$  in (8b) is explicitly re-described as follows:

$$\Pr\left\{B \log_2\left(1 + \frac{|g_l^H|^2 p_l}{\sum_{i=l+1}^L |g_i^H|^2 p_i + BN_0}\right) \geq r_l\right\} = \Pr\left\{g_l^H \Phi_l g_l - BN_0 \geq 0\right\} \tag{10}$$

where  $\Phi_l = \frac{p_l}{2^{\frac{r_l}{B}} - 1} - \sum_{i=l+1}^L p_i$ .

For convenience, we assume that  $\Sigma_l = \varepsilon_l^2 \mathbf{I}$ , then the error defined in (5) can be rewritten as  $\text{vec}(\Delta g_l) = \varepsilon_l i_l$ , where  $i_l = \mathcal{CN}(0, \mathbf{I})$ . Then the rate OP constraints (8) can be reformulated as follows:

$$\begin{aligned} & \Pr\left\{g_l^H \Phi_l g_l^H - BN_0 \geq 0\right\} \\ &= \Pr\left\{\text{vec}^H(\Delta g_l) \Phi_l \text{vec}(\Delta g_l) + 2 \text{Re}\left\{\text{vec}\left(\hat{g}_l^H \Phi_l\right) \text{vec}(\Delta g_l)\right\} + \hat{g}_l^H \Phi_l \hat{g}_l - BN_0 \geq 0\right\} \downarrow \\ &= \Pr\left\{\varepsilon_l^2 i_l^H \Phi_l i_l + 2 \text{Re}\left\{\varepsilon_l \text{vec}\left(\hat{g}_l^H \Phi_l\right) i_l\right\} + \hat{g}_l^H \Phi_l \hat{g}_l - BN_0 \geq 0\right\}. \end{aligned} \tag{11}$$

Substitute (11) into (8b). According to Lemma 1, the rate OP constraints (8b) in (8) are given as follows

$$\Pr\left\{i_l^H \mathbf{U}_l i_l + 2 \text{Re}\left\{\mathbf{u}_l^H i_l\right\} + v_l \geq 0\right\} \geq 1 - \rho_l, \tag{12}$$

where

$$\begin{aligned} \mathbf{U}_l &= \varepsilon_l^2 \Phi_l \\ \mathbf{u}_l &= \varepsilon_l \text{vec}\left(\hat{g}_l^H \Phi_l\right) \\ v_l &= \hat{g}_l^H \Phi_l \hat{g}_l - BN_0. \end{aligned}$$

Apply Lemma 1 presented above to the equivalent transformation of expression (12). First, we introduce two auxiliary variables  $\mathbf{s} = [s_1, \dots, s_l]^T$  and  $\mathbf{t} = [t_1, \dots, t_l]^T$ , and then according to equation (9), constraint (12) can be equivalent to the following deterministic form:

$$\text{Tr}\{\mathbf{U}_l\} - \sqrt{2 \ln(1/\rho_l)} s_l - \ln(\rho_l) t_l + v_l \geq 0 \tag{13a}$$

$$\sqrt{\|\mathbf{U}_l\|_F^2 + 2\|\mathbf{u}_l\|^2} \leq s_l \tag{13b}$$

$$t_l \mathbf{I} + \mathbf{U}_l \succeq 0, t_l \geq 0, \tag{13c}$$

(13) can be simplified by the following series of mathematical transformations:

$$\text{Tr}\{\mathbf{U}_l\} = \varepsilon_l^2 \text{Tr}(\Phi_l) = \varepsilon_l^2 \text{Tr}(\Phi_l) \text{Tr}(E) = \varepsilon_l^2 \text{Tr}(\Phi_l) \tag{14a}$$

$$\|\mathbf{U}_l\|_F^2 = \varepsilon_l^4 \|\Phi_l\|_F^2 \tag{14b}$$

$$\|\mathbf{u}_l\|^2 = \varepsilon_l^2 \left\| \hat{g}_l^H \Phi_l \right\|_2^2, \tag{14c}$$

$$\lambda(\mathbf{U}_l) = \lambda\left(\varepsilon_l^2 \Phi_l\right) = \varepsilon_l^2 \lambda(\Phi_l), \tag{14d}$$

where  $\lambda(\mathbf{U}_l)$  represents the eigenvalue operation of  $\mathbf{U}_l$ . According to (13) and (14), constraint (8b) can be converted to the following form:

$$\varepsilon_l^2 \text{Tr}(\Phi_l) - \sqrt{2 \ln(1/\rho_l)} s_l - \ln(\rho_l) t_l + v_l \geq 0, \forall l \in \mathcal{L} \tag{15a}$$

$$\left\| \begin{matrix} \varepsilon_l^2 \text{vec}(\Phi_l) \\ \sqrt{2} \varepsilon_l \Phi_l \hat{g}_l \end{matrix} \right\| \leq s_l, \forall l \in \mathcal{L} \tag{15b}$$

$$t_l \mathbf{I} + \varepsilon_l^2 \Phi_l \succeq 0, t_l \geq 0, \forall l \in \mathcal{L} \tag{15c}$$

Replace constraint (8b) with expression (15) equivalent, then the equivalent form of optimization problem (8) is as follows:

$$\begin{aligned} & \min_{p,s,t} \sum_{l=1}^L p_l & (16a) \\ \text{s.t. } & \varepsilon_l^2 \text{Tr}(\Phi_l) - \sqrt{2 \ln(1/\rho_l)} s_l - \ln(\rho_l) t_l + v_l \geq 0, \forall l \in \mathcal{L} & (16b) \\ & \left\| \frac{\varepsilon_l^2 \text{vec}(\Phi_l)}{\sqrt{2\varepsilon_l} \Phi_l \hat{g}_l} \right\| \leq s_l, \forall l \in \mathcal{L} & (16c) \\ & t_l \mathbf{I} + \varepsilon_l^2 \Phi_l \geq 0, t_l \geq 0, \forall l \in \mathcal{L} & (16d) \\ & p_i \geq p_l, \forall i < l & (16e) \\ & |g_1^H| \leq \dots \leq |g_L^H|. & (16f) \end{aligned}$$

After the equivalent transformation, problem (16) is still complicated due to its non-convex.

### 3.3. Matrix Lifting

To solve non-convex problem (16), we redescribe the optimization problem as SDP by matrix lifting. We denote  $P_l = \sqrt{p_l} \sqrt{p_l}^H$ , which is a symmetric positive semi-definite (PSD) matrix of rank one. Then, problem (16) can be equivalent as follows:

$$\begin{aligned} \mathcal{P}_A : & \min_{p,s,t} \sum_{l=1}^L \text{Tr}\{P_l\} & (17a) \\ \text{s.t. } & \varepsilon_l^2 \text{Tr}(\Phi_l) - \sqrt{2 \ln(1/\rho_l)} s_l - \ln(\rho_l) t_l + v_l \geq 0, \forall l \in \mathcal{L} & (17b) \\ & \left\| \frac{\varepsilon_l^2 \text{vec}(\Phi_l)}{\sqrt{2\varepsilon_l} \Phi_l \hat{g}_l} \right\| \leq s_l, \forall l \in \mathcal{L} & (17c) \\ & t_l \mathbf{I} + \varepsilon_l^2 \Phi_l \geq 0, t_l \geq 0, \forall l \in \mathcal{L} & (17d) \\ & P_l \geq 0, \forall l \in \mathcal{L} & (17e) \\ & \text{rank}(P_l) = 1, \forall l \in \mathcal{L} & (17f) \\ & p_i \geq p_l, \forall i < l & (17g) \\ & |g_1^H| \leq \dots \leq |g_L^H|. & (17h) \end{aligned}$$

After restating problem (16) as an SDP problem, we can deal with the nonconvexity in problem (17) via the SDR technique [40], i.e., ignoring  $\text{rank}(P_l) = 1, \forall l \in \mathcal{L}$  from problem (14). The SDP problem obtained can be effectively resolved by using the CVX tool [41]. It is worth noting that if the solution obtained satisfies the rank 1 constraint, the optimal solution of the original problem can be obtained through Cholesky decomposition. Otherwise, if the solution obtained by the SDR method does not meet rank 1, the Gaussian randomization method should be used to obtain the suboptimal solution [40]. Summarily, the SDR method for solving problem  $\mathcal{P}_A$  is summarized in Algorithm 1.



**Algorithm 1:** SDR Algorithm for Problem  $\mathcal{P}_A$ .

---

```

1: Input random initial value  $p_l^0$ , set predefined threshold  $\epsilon > 0$ .
2: Output  $\mathbf{P}^*$ .
3: for  $t \leftarrow 1, 2, \dots$ , do
4:   Solve the problem  $\mathcal{P}_A$ , to get  $\mathbf{P}^t$ .
5:   if  $\left| \sum_{l=1}^L \text{Tr}\{\mathbf{P}_l^t\} - \sum_{l=1}^L \text{Tr}\{\mathbf{P}_l^{t-1}\} \right| < \epsilon$ , then
6:      $\mathbf{P}^* = \mathbf{P}^t$ .
7:     if  $\text{rank}(\mathbf{P}^*) = 1$ , then
8:       Cholesky decomposition for  $\mathbf{P}^* = \sqrt{p_l} \sqrt{p_l}^H$  to obtain  $p_l^*$ .
9:     break
10:    else
11:      Gaussian randomization to obtain  $p_l^*$ 
12:    break
13:    end
14:  end
15: end

```

---

**4. Simulation Results and Analysis**

In this section, we provide the simulation results of optimizing the total transmit power for NOMA-based D2D offloading systems in the presence of CSI estimation error. We compare the numerical results of NOMA and OMA multiple access. We analyze the influence of CSI estimation error on system performance.

**4.1. Simulation Settings**

In the simulations, we assume that transmit users of the D2D system are evenly distributed in a circle with (0,0 m) as the center and a radius of 3 m, and receive users of the D2D system are evenly distributed in a circle with (30,0 m) as the center and a radius of 3 m. Here, we assume that the channel model includes small-scale fading and large-scale fading. Here, we assume small-scale fading obeys Rayleigh distribution, and the model of large-scale fading is defined as  $PL = -30 - 10\alpha \log_{10}(d) \text{ dB}$ , where  $\alpha$  represent the link loss index and  $d$  represent the link distance between transmit users and receive users. For the CSI statistical error model in this paper, the variance of  $\text{vec}(\Delta g_l)$  is defined as  $\Sigma_l^2 = \gamma^2 |\text{vec}(\hat{g}_l)|^2$ ,  $\gamma \in [0, 1)$  measures the degree of CSI uncertainty. We assume that the minimum constraint rates are the same for all users, i.e.,  $r_1 = \dots = r_L = r$ , and we also assume that the rate OP thresholds are the same for all users, i.e.,  $\rho_1 = \dots = \rho_L = \rho$ . The settings of simulation parameters are shown in Table 1.

**Table 1.** Settings of simulation parameters.

Parameter	Value
link loss index of users	$\alpha = 2$
Noise power	$\{\sigma^2\}_{l=1}^L = -80 \text{ dBm}$
Convergence tolerance	$\epsilon = 10^{-4}$
Communication bandwidth	$B = 10^7 \text{ Hz}$

**4.2. Results Analysis**

Figure 3 illustrates the minimum transmit power versus the rate OP threshold when the communication channel is imperfect. We assume user pairs  $L = 2$ , and the degree of CSI uncertainty  $\gamma = 0.02$ . As the rate OP threshold increases, the transmit power in all cases decreases significantly, indicating that the lower the communication quality of the system, the less transmit power required by the NOMA-aided D2D system. From Figure 3, we can also observe that the higher the minimum rate of user communication, the greater the transmission power required by the system. The reason is that the system needs more

power to improve the communication quality of the NOMA-based D2D system. That is, there is a trade-off between the communication quality and transmit power.

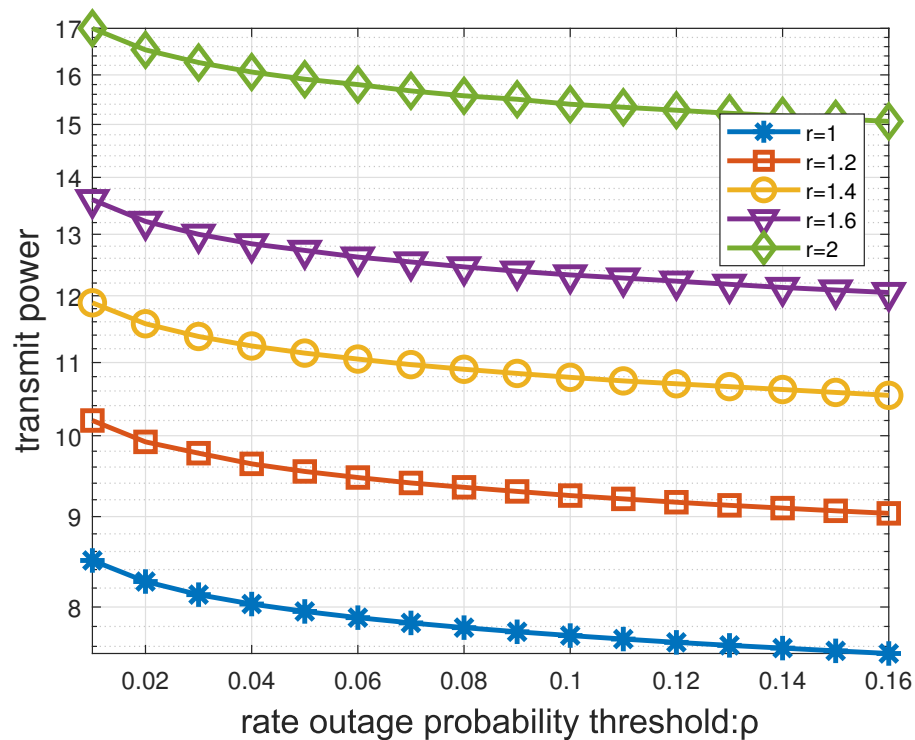


Figure 3. Transmit power versus the rate outage probability threshold  $\rho$ , when  $L = 2, \gamma = 0.02$ .

Figure 4 illustrates the minimum transmit power versus minimum rate constraint  $r$  for all users when the communication channel is imperfect. We assume user pairs  $L = 2$  and the rate OP threshold  $\rho = 0.05$ . From Figure 4, we can observe that as the channel estimation error increases, the transmit power required by the system also increases. This is because the system needs to spend more transmit power to compensate for the rate loss caused by channel errors. In Figure 4, we also compared the total transmit power of the system under NOMA and OMA. As shown in Figure 4, the transmitting power of the OMA communication mode is much higher than that of the NOMA communication mode under the same system parameters. This is because NOMA allows all node users to use all spectrum resources at the same time, which greatly improves spectrum efficiency. It is verified in Figure 3 that there is a trade-off between the system's transmit power and the user's transmit rate. So, NOMA can significantly save system power compared to OMA at the same transmission rate.

Figure 5 illustrates the minimum transmit power versus user pairs  $L$  when the communication channel is imperfect. We assume the degree of CSI uncertainty  $\gamma = 0.02$  and the rate OP threshold  $\rho = 0.05$ . As can be seen from Figure 5, the transmit power of the system increases sharply with the increase in the number of user pairs. The rapid increase in nodes in the IoT will greatly increase the power consumption of the communication system, so the power optimization of the communication system becomes a non-negligible problem. Figure 5 also illustrates that NOMA multiple access can improve system performance better than OMA. This is because NOMA technology can greatly improve the spectral efficiency of the system, which can accommodate more users under the same channel bandwidth.

Figure 6 illustrates the minimum transmit power versus statistical CSI error  $\gamma$  when the communication channel is imperfect. We assume user pairs  $L = 2$  and the rate OP threshold  $\rho = 0.05$ . From Figure 6, we can observe that the transmit power of the system increases with the increase in the user's minimum constraint rate, indicating that the system needs more power to ensure the user's transmission rate. So, there is a trade-off between

system power consumption and user speed. We can also see from Figure 6 that the transmit power of OMA communication is much higher than that of NOMA. This is because NOMA technology has a much higher spectral efficiency than OMA, which better compensates for user rate losses due to channel errors.

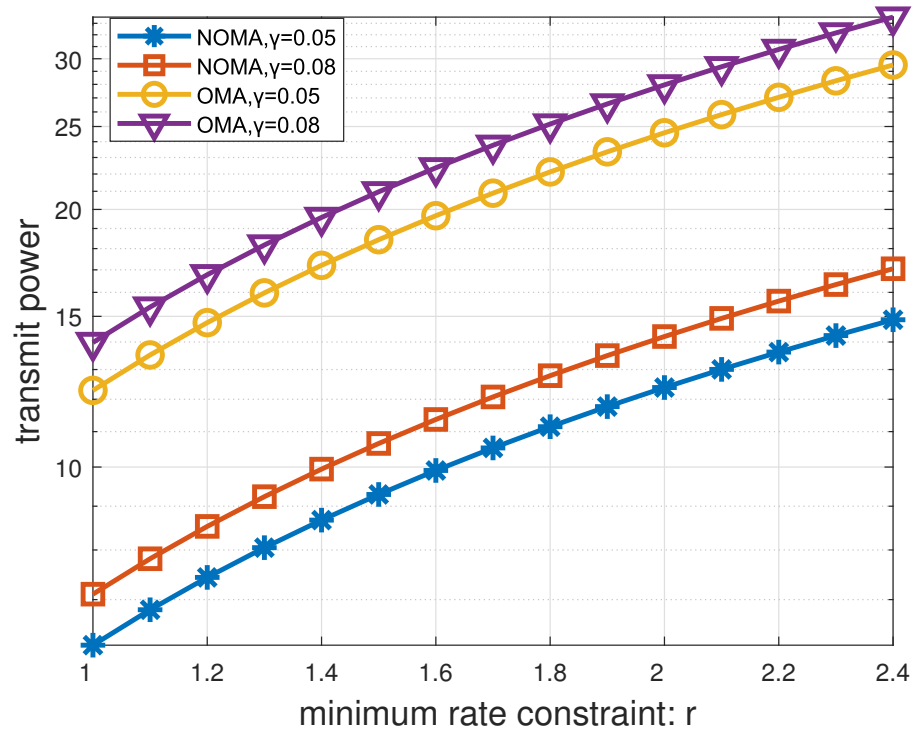


Figure 4. Transmit power versus minimum rate constraint  $r$ , when  $L = 2, \rho = 0.05$ .

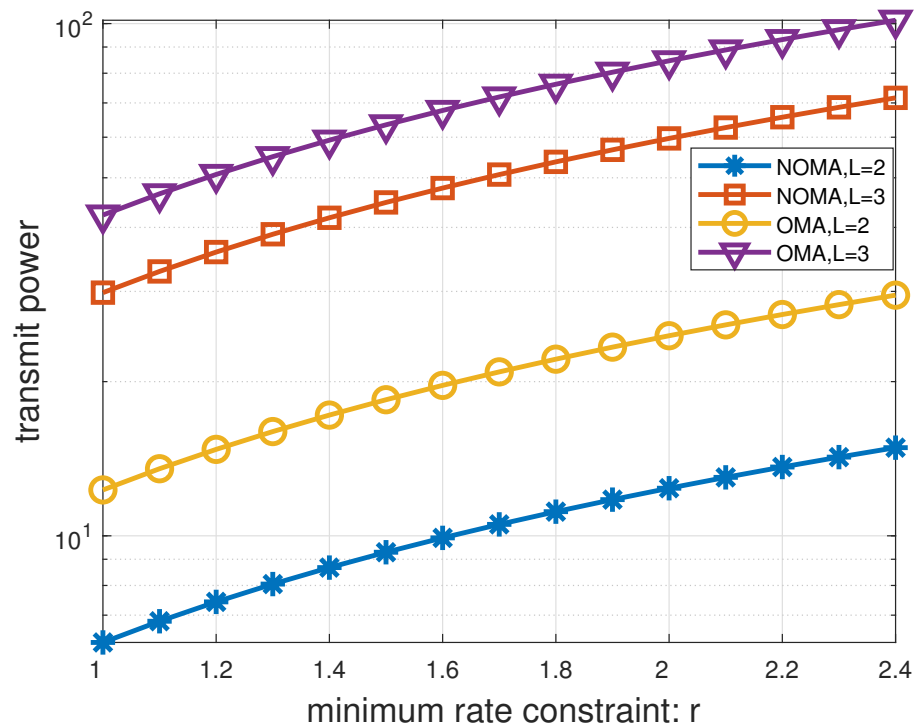


Figure 5. Transmit power versus minimum rate constraint  $r$ , when  $\gamma = 0.02, \rho = 0.05$ .

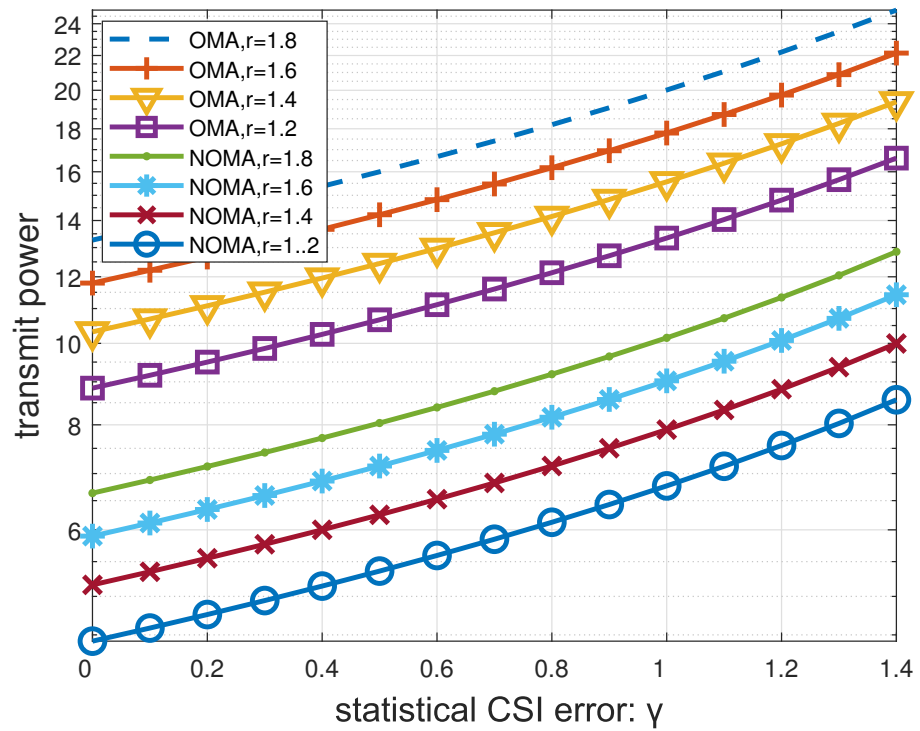


Figure 6. Transmit power versus statistical CSI error, when  $L = 2, \rho = 0.05$ .

We measure system outage in terms of feasibility rate. Specifically, we define the feasibility rate as the ratio of the feasible channel number to the total channel number subject to the rate OP of user, in which the feasible channel refers to the feasible solution of rate OP constraint optimization problem (8). Figure 7 shows the feasibility rate of the D2D system versus rate outage probability threshold  $\rho$ . From Figure 7, we can find that the probability of communication outage is consistent with the preset rate outage probability threshold, which also verifies the effectiveness of our proposed algorithm.

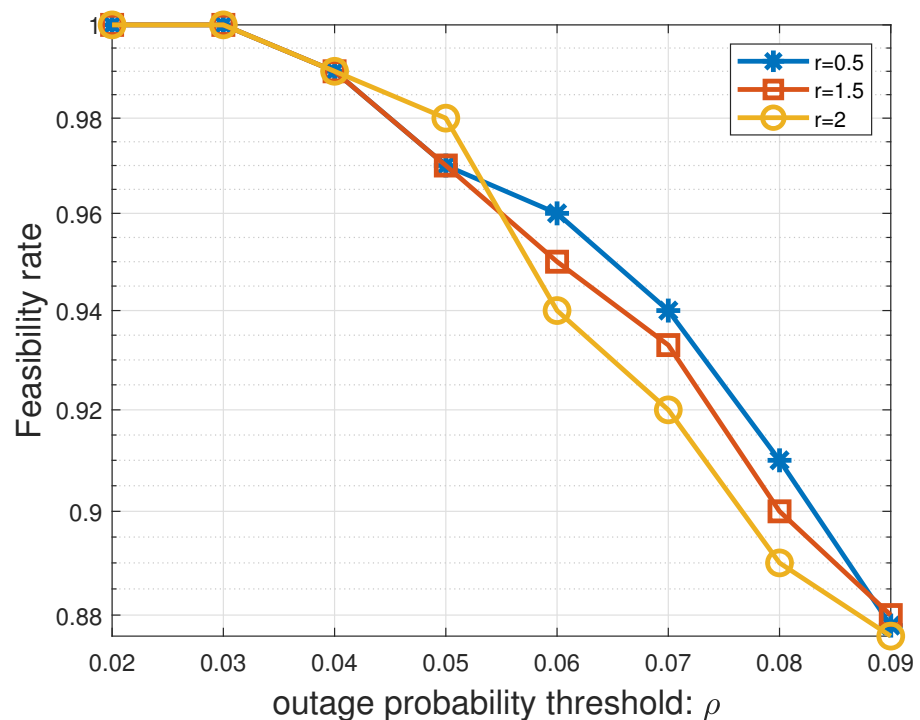


Figure 7. Feasibility rate versus rate outage probability threshold  $\rho$ , when  $L = 2$ .

## 5. Conclusions

In this paper, NOMA communication is suggested to assist D2D communication in saving system bandwidth and improving communication efficiency. We investigated and analyzed the robust beamforming design under imperfect CSI of the NOMA-based D2D offloading systems. We considered the influence of CSI uncertainty on the beamforming design. Our goal was to optimize the system transmit power under the rate OP constraint under the CSI statistical error model. The results show that the larger the channel estimation error, the greater the system power consumption. We also compared the impact of NOMA and OMA on the system, and the numerical results show that NOMA multiple access can improve system performance better than OMA.

**Author Contributions:** Conceptualization, Y.C., G.Z. and H.X.; formal analysis, Y.C. and G.Z.; funding acquisition, H.X. and Y.R.; investigation, G.Z. and H.X.; methodology, Y.C. and H.X.; resources, G.Z.; software, Y.C.; validation, Y.C.; writing—original draft, Y.C.; writing—review and editing, Y.R., X.C. and R.L. All authors have read and agreed to the published version of the manuscript.

**Funding:** This work is funded by the Fundamental Research Funds for the Central Universities (No. CCNU20TS008); The Science and Technology Department of Guizhou Province Project (No.[2020]1Y208); The Guizhou Provincial Department of Education Project (No.KY[2020]208); and Qiannan Normal College for Nationalities Project (No. QNSY2018002, 2018XJG0530).

**Data Availability Statement:** The code used to support the findings of this study is available at the following <https://github.com/chenyun85> (accessed on 10 November 2021).

**Conflicts of Interest:** The authors declare no conflict of interest.

## References

1. Han, T.; Ge, X.; Wang, L.; Kwak, K.S.; Han, Y.; Liu, X. 5G Converged Cell-Less Communications in Smart Cities. *IEEE Commun. Mag.* **2017**, *55*, 44–50. [\[CrossRef\]](#)
2. Li, C.; Zhang, S.; Liu, P.; Sun, F.; Cioffi, J.M.; Yang, L. Overhearing Protocol Design Exploiting Intercell Interference in Cooperative Green Networks. *IEEE Trans. Veh. Technol.* **2016**, *65*, 441–446. [\[CrossRef\]](#)
3. Ali, M.S.; Hossain, E.; Kim, D.I. LTE/LTE-A Random Access for Massive Machine-Type Communications in Smart Cities. *IEEE Commun. Mag.* **2017**, *55*, 76–83. [\[CrossRef\]](#)
4. Li, C.; Liu, P.; Zou, C.; Sun, F.; Cioffi, J.M.; Yang, L. Spectral-Efficient Cellular Communications With Coexistent One- and Two-Hop Transmissions. *IEEE Trans. Veh. Technol.* **2016**, *65*, 6765–6772. [\[CrossRef\]](#)
5. Kim, J.B.; Lee, I.H.; Lee, J. Capacity Scaling for D2D Aided Cooperative Relaying Systems Using NOMA. *IEEE Wirel. Commun. Lett.* **2018**, *7*, 42–45. [\[CrossRef\]](#)
6. Chen, J.; Jia, J.; Liu, Y.; Wang, X.; Aghvami, A.H. Optimal Resource Block Assignment and Power Allocation for D2D-Enabled NOMA Communication. *IEEE Access* **2019**, *7*, 90023–90035. [\[CrossRef\]](#)
7. Mao, Y.; You, C.; Zhang, J.; Huang, K.; Letaief, K.B. A Survey on Mobile Edge Computing: The Communication Perspective. *IEEE Commun. Surv. Tutor.* **2017**, *19*, 2322–2358. [\[CrossRef\]](#)
8. Hu, W.; Cao, G. Quality-Aware Traffic Offloading in Wireless Networks. *IEEE Trans. Mob. Comput.* **2017**, *16*, 3182–3195. [\[CrossRef\]](#)
9. Tao, Y.; You, C.; Zhang, P.; Huang, K. Stochastic Control of Computation Offloading to a Helper With a Dynamically Loaded CPU. *IEEE Trans. Wirel. Commun.* **2019**, *18*, 1247–1262. [\[CrossRef\]](#)
10. Diao, X.; Zheng, J.; Wu, Y.; Cai, Y. Joint Computing Resource, Power and Channel Allocations for D2D-Assisted and NOMA-based Mobile Edge Computing. *IEEE Access* **2019**, *7*, 9243–9257. [\[CrossRef\]](#)
11. He, Y.; Ren, J.; Yu, G.; Cai, Y. D2D Communications Meet Mobile Edge Computing for Enhanced Computation Capacity in Cellular Networks. *IEEE Trans. Wirel. Commun.* **2019**, *18*, 1750–1763. [\[CrossRef\]](#)
12. Jameel, F.; Hamid, Z.; Jabeen, F.; Zeadally, S.; Javed, M.A. A Survey of Device-to-Device Communications: Research Issues and Challenges. *IEEE Commun. Surv. Tutor.* **2018**, *20*, 2133–2168. [\[CrossRef\]](#)
13. Chukhno, N.; Trilles, S.; Torres-Sospedra, J.; Iera, A.; Araniti, G. D2D-based Cooperative Positioning Paradigm for Future Wireless Systems: A Survey. *IEEE Sens. J.* **2021**. [\[CrossRef\]](#)
14. Wang, F.; Xu, C.; Song, L.; Han, Z. Energy-Efficient Resource Allocation for Device-to-Device Underlay Communication. *IEEE Trans. Wirel. Commun.* **2015**, *14*, 2082–2092. [\[CrossRef\]](#)
15. Jiang, Y.; Liu, Q.; Zheng, F.; Gao, X.; You, X. Energy-Efficient Joint Resource Allocation and Power Control for D2D Communications. *IEEE Trans. Veh. Technol.* **2016**, *65*, 6119–6127. [\[CrossRef\]](#)
16. Lin, S.; Ding, H.; Fang, Y.; Shi, J. Energy-Efficient D2D Communications With Dynamic Time-Resource Allocation. *IEEE Trans. Veh. Technol.* **2019**, *68*, 11985–11999. [\[CrossRef\]](#)

17. Najla, M.; Becvar, Z.; Mach, P.; Gesbert, D. Predicting Device-to-Device Channels From Cellular Channel Measurements: A Learning Approach. *IEEE Trans. Wirel. Commun.* **2020**, *19*, 7124–7138. [[CrossRef](#)]
18. Liu, Y.; Hu, Q.; Cai, Y.; Juntti, M. Latency Minimization in Intelligent Reflecting Surface Assisted D2D Offloading Systems. *IEEE Commun. Lett.* **2021**, *25*, 3046–3050. [[CrossRef](#)]
19. Zhou, Z.; Ota, K.; Dong, M.; Xu, C. Energy-Efficient Matching for Resource Allocation in D2D Enabled Cellular Networks. *IEEE Trans. Veh. Technol.* **2017**, *66*, 5256–5268. [[CrossRef](#)]
20. Kuang, Z.; Liu, G.; Li, G.; Deng, X. Energy Efficient Resource Allocation Algorithm in Energy Harvesting-Based D2D Heterogeneous Networks. *IEEE Internet Things J.* **2019**, *6*, 557–567. [[CrossRef](#)]
21. Sawyer, N.; Smith, D.B. Flexible Resource Allocation in Device-to-Device Communications Using Stackelberg Game Theory. *IEEE Trans. Commun.* **2019**, *67*, 653–667. [[CrossRef](#)]
22. Saito, Y.; Kishiyama, Y.; Benjebbour, A.; Nakamura, T.; Higuchi, K. Non-Orthogonal Multiple Access (NOMA) for Cellular Future Radio Access. In Proceedings of the 2013 IEEE 77th vehicular technology conference (VTC Spring), Dresden, Germany, 2–5 June 2013; pp. 1–5.
23. Saito, Y.; Benjebbour, A.; Kishiyama, Y.; Nakamura, T. System-level performance evaluation of downlink non-orthogonal multiple access (NOMA). In Proceedings of the 2013 IEEE 24th Annual International Symposium on Personal, Indoor, and Mobile Radio Communications (PIMRC), London, UK, 8–11 September 2013; pp. 611–615. [[CrossRef](#)]
24. Di, B.; Song, L.; Li, Y. Sub-Channel Assignment, Power Allocation, and User Scheduling for Non-Orthogonal Multiple Access Networks. *IEEE Trans. Wirel. Commun.* **2016**, *15*, 7686–7698. [[CrossRef](#)]
25. Sun, Y.; Ng, D.W.K.; Ding, Z.; Schober, R. Optimal Joint Power and Subcarrier Allocation for Full-Duplex Multicarrier Non-Orthogonal Multiple Access Systems. *IEEE Trans. Commun.* **2017**, *65*, 1077–1091. [[CrossRef](#)]
26. Ding, Z.; Schober, R.; Poor, H.V. A General MIMO Framework for NOMA Downlink and Uplink Transmission Based on Signal Alignment. *IEEE Trans. Wirel. Commun.* **2016**, *15*, 4438–4454. [[CrossRef](#)]
27. Ding, Z.; Poor, H.V. Design of Massive-MIMO-NOMA With Limited Feedback. *IEEE Signal Process. Lett.* **2016**, *23*, 629–633. [[CrossRef](#)]
28. Liu, M.; Song, T.; Gui, G. Deep Cognitive Perspective: Resource Allocation for NOMA-Based Heterogeneous IoT With Imperfect SIC. *IEEE Internet Things J.* **2019**, *6*, 2885–2894. [[CrossRef](#)]
29. Bai, W.; Yao, T.; Zhang, H.; Leung, V.C.M. Research on Channel Power Allocation of Fog Wireless Access Network Based on NOMA. *IEEE Access* **2019**, *7*, 32867–32873. [[CrossRef](#)]
30. Sun, M.; Xu, X.; Tao, X.; Zhang, P.; Leung, V.C.M. NOMA-Based D2D-Enabled Traffic Offloading for 5G and Beyond Networks Employing Licensed and Unlicensed Access. *IEEE Trans. Wirel. Commun.* **2020**, *19*, 4109–4124. [[CrossRef](#)]
31. Li, J.; Li, X.; Wang, A.; Ye, N. BeamSpace MIMO-NOMA for Millimeter-Wave Broadcasting via Full-Duplex D2D Communications. *IEEE Trans. Broadcast.* **2020**, *66*, 545–554. [[CrossRef](#)]
32. Pan, Y.; Pan, C.; Yang, Z.; Chen, M. Resource Allocation for D2D Communications Underlying a NOMA-Based Cellular Network. *IEEE Wirel. Commun. Lett.* **2018**, *7*, 130–133. [[CrossRef](#)]
33. Madani, N.; Sodagari, S. Performance Analysis of Non-Orthogonal Multiple Access With Underlaid Device-to-Device Communications. *IEEE Access* **2018**, *6*, 39820–39826. [[CrossRef](#)]
34. Zhao, J.; Liu, Y.; Chai, K.K.; Chen, Y.; ElKashlan, M. Joint Subchannel and Power Allocation for NOMA Enhanced D2D Communications. *IEEE Trans. Commun.* **2017**, *65*, 5081–5094. [[CrossRef](#)]
35. Le, C.B.; Do, D.T. Joint evaluation of imperfect SIC and fixed power allocation scheme for wireless powered D2D-NOMA networks with multiple antennas at base station. *Wirel. Netw.* **2019**, *25*, 5069–5081. [[CrossRef](#)]
36. Duan, W.; Ji, Y.; Hou, J.; Zhuo, B.; Wen, M.; Zhang, G. Partial-DF Full-Duplex D2D-NOMA Systems for IoT With/Without an Eavesdropper. *IEEE Internet Things J.* **2021**, *8*, 6154–6166. [[CrossRef](#)]
37. Chen, Y.; Zhang, G.; Xu, H.; Chen, X.; Li, R. Federated Learning: Sum Power Constraints Optimization Design. *Arab. J. Sci. Eng.* **2021**. [[CrossRef](#)]
38. Hassan, A.K.; Moinuddin, M.; Al-Saggaf, U.M.; Aldayel, O.; Davidson, T.N.; Al-Naffouri, T.Y. Performance Analysis and Joint Statistical Beamformer Design for Multi-User MIMO Systems. *IEEE Commun. Lett.* **2020**, *24*, 2152–2156. [[CrossRef](#)]
39. Wang, K.Y.; So, A.M.C.; Chang, T.H.; Ma, W.K.; Chi, C.Y. Outage Constrained Robust Transmit Optimization for Multiuser MISO Downlinks: Tractable Approximations by Conic Optimization. *IEEE Trans. Signal Process.* **2014**, *62*, 5690–5705. [[CrossRef](#)]
40. Luo, Z.Q.; Ma, W.K.; So, M.C.; Ye, Y.; Zhang, S. Semidefinite Relaxation of Quadratic Optimization Problems. *IEEE Signal Process. Mag.* **2010**, *27*, 20–34. [[CrossRef](#)]
41. Grant, M. CVX: MATLAB Software for Disciplined Convex Programming. 2008. Available online: <http://cvxr.com/cvx> (sccessed on 5 November 2021).